A GNC Algorithm for Deblurring Images with Interacting Discontinuities

A. Boccuto, M. Discepoli, I. Gerace, R. Pandolfi, P. Pucci

Dipartimento di Matematica e Informatica, Università degli Studi di Perugia.

via Vanvitelli 1 Perugia, Italy. *E-mail: gerace@dipmat.unipg.it*

Abstract

In this paper we present a Graduated Non-Convexity (GNC) algorithm for reconstructing images. We assume that the data images are blurred and corrupted by white Gaussian noise. Geometric features of discontinuities are introduced in the model and the problem is formulated as the minimization of a non-convex function. We give a convex approximation of such a function and a family of approximating functions. Moreover, to analize the convex approximation, we prove an alternative duality theorem to implicitly treat discontinuities of images. The experimental results are more satisfactory than those obtained by some standard algorithms.

Introduction

In this paper we deal with the problem of image restoration. In particular we assume to have an image blurred by a known operator and corrupted by an independent Gaussian white noise with zero mean and known variance. Our goal is to estimate from the observed image the original one. It is well-known that this is a typical ill-posed inverse problem in the sense of Hadamard; so, in order to solve this problem, some regularization techniques were proposed [1, 3, 4, 9]. In this paper we assume that restored images will be piecewise smooth; moreover we make an estimate of unknown discontinuities. A solution is defined as the minimum of the so-called *primal energy function,* which is the sum of two terms: the former is a measure of faithfulness of the solution to data, and the latter controls the degree of smoothness of the solution. In the case of image deblurring, an important constraint to give to the solution is

that close discontinuities must be not parallel: therefore, to this aim, we add a suitable term to the primal energy function. The *dual energy function* is the energy function that deal implicitly with discontinuities. Geman and Reynolds [11] and Charbonnier, Blanc-Féraud, Aubert and Barlaud [8] gave two different versions of the duality theorem: this theorem gives a correspondence between primal and dual energy functions. In this paper we present a new version of the duality theorem, with stronger conditions and at the same time more flexible to real applications. For the sake of shortness, we refer to [7] for the proof of such theorem. A classical technique for minimizing the dual energy function is the GNC (Graduated Non-Convexity) algorithm [2, 5, 6, 12]; to apply this, it is necessary to give a family of approximations of the dual energy. The first approximation should be convex and the last one is the original function. Each approximation is minimized by starting from the minimum point of the previous one. In this paper we present a new family of approximating functions, for the problem of deblurring, which takes into account the constraint of non-parallelism of discontinuities. We call CATILED (Convex Approximation Technique for Interacting Line Elements Deblurring) the GNC algorithm that uses such kind of approximating functions. Moreover, by the duality theorem, we show that the first convex approximation of CATILED corresponds to a primal energy that adequately treats the involved discontinuities.

The experimental results show how CATILED recovers discontinuity of restored image, better than some classical GNC algorithms. In Section 1 we present the problem of image restoration; in Section 2 we show how to deal with geometry of discontinuities; in Section 3 we define the dual energy and we present the duality theorem; in Section 4 we explain the GNC technique; in Section 5 we define the CATILED algorithm; in Section 6 we find the primal energy function of the first convex approximation of CATILED; in Section 7 we give some experimental results.

1 The problem of image restoration

The aim of our problem is to reconstruct the original image from an image blurred and/or corrupted by noise. The direct problem can be formulated as follows:

$$\boldsymbol{y} = A\boldsymbol{x} + \boldsymbol{n},$$

where the vectors $\boldsymbol{x}$, $\boldsymbol{y}$ are respectively the original image and the observed one. The vector $\boldsymbol{n}$ is a white Gaussian noise on the image, and the $n^2 \times n^2$

matrix A is a linear operator, which represents the blur acting on the image. All the involved vectors are n^2 size and are considered in lexicographic order. To obtain a blurred image from the original, each pixel of destination image is set to a weighted average of the corresponding pixel in original image and its neighbours. Given a positive matrix $M \in \mathbb{R}^{(2h+1)\times(2h+1)}$, called *blur mask,* such that $\sum_{i,j} m_{i,j} = 1$, we define A as $a_{(i,j),(i+w,j+v)} = m_{h+1+w,h+1+v}$ if $1 \leq h+1+w \leq 2h+1$ and $1 \leq h+1+v \leq 2h+1$, and $a_{(i,j),(i+w,j+v)} = 0$ otherwise. The image restoration problem is the following inverse problem: given the blurred image $\boldsymbol{y}$, the matrix A and the variance of the noise, find an estimation $\boldsymbol{x}$ of the original image.
We now introduce some auxiliary variables associated to discontinuity of the image $\boldsymbol{x}$. A good estimate of the discontinuity improves the quality of the restored image.

Given a fixed number $n \in I\!N$, let $Q_n = ([1,n] \cap I\!N) \times ([1,n] \cap I\!N)$. We call *clique* of order k the set of points of Q_n on which the finite difference of order k is defined. We indicate with the symbol C_k the set of all cliques of order k. For example, $C_1 = \{c = \{(i,j),(h,l)\} : i = h, j = l+1 \,\text{or}\, i = h+1, j = l\}$, and in this case we denote the finite difference operator of order k of the vector $\boldsymbol{x}$ associated with the clique c by $D_c^k \boldsymbol{x}$. For example, $D_c^1 \boldsymbol{x} = x_{i,j} - x_{h,l}$, if $c = \{(i,j),(h,l)\} \in C_1$.

We now associate to every clique c a weight $b_c \in [0, +\infty)$, which we call *line variable.* A small value of b_c corresponds to a suitable discontinuity of our involved image in c. We define the vector $\boldsymbol{b}$ as the set of all components b_c, $c \in C_k$, with $k \in I\!N$ fixed.

It is well-known that the image restoration problem is ill-posed in the sense of Hadamard [3, 4, 9]. By regularization techniques [1, 8, 11] we can define the solution of the problem as the minimum of the following function, called *primal energy function* :

$$E(\boldsymbol{x}, \boldsymbol{b}) = \|\boldsymbol{y} - A\boldsymbol{x}\|^2 + \sum_{c \in C_k} \left[\lambda^2 (D_c^k \boldsymbol{x})^2 b_c + \beta(b_c)\right], \tag{1}$$

where the first term measures faithfulness of the solution to data and the second one is a regularization term, which imposes a smoothness condition on $\boldsymbol{x}$ of order k. Here λ^2, called *regularization parameter,* reflects the confidence that we have in the data. Let us assume β to be a strictly decreasing function, in order to avoid to have too many discontinuities in the restored image. A suitable choice of k allows us to obtain piecewise constant ($k = 1$), linear ($k = 2$) or quadratic ($k = 3$) restored images.

Throughout this paper, we often refer to the following case [2, 5, 6, 10, 12]:

$$B = \{0, 1\}, \qquad \beta(b) = \alpha(1 - b), \tag{2}$$

where α is a suitable positive parameter.

2 Geometry of discontinuities

We consider a new term, $Q(\boldsymbol{b})$, which is added to the energy function in (1), in order to have suitable geometric features of discontinuities of the restored image.
Given a partition Π of C_k, let us define a total ordering $\preceq$ on each element π of Π. Given two elements c_1, c_2 belonging to the same element π of the partition Π, we write $c_1 = c_2 - 1$ if c_2 covers c_1. We assume that Q is of the following type:

$$Q(\boldsymbol{b}) = \sum_{c \in \Gamma} \rho(b_c, b_{c-1}), \tag{3}$$

where $\Gamma = \bigcup_{\pi \in \Pi}(\pi \setminus \min \pi)$ and ρ is a suitable function, depending on the geometry of the discontinuity we are considering. For example, if we want to avoid parallel discontinuities, a possible partition of C_1 is $\Pi = \Pi_1 \cup \Pi_2$, where $\Pi_1 = \{\{(i, j), (i-1, j)\colon 2 \leq i \leq n\}\colon 1 \leq j \leq n\}$ and $\Pi_2 = \{\{(i, j), (i, j-1)\colon 2 \leq j \leq n\} : 1 \leq i \leq n\}$. The corresponding order on each $\pi_1 \in \Pi_1$ is $\{(i, j), (i - 1, j)\} \preceq \{(h, j), (h-1, j)\}$ iff $i \leq h$, and on every $\pi_2 \in \Pi_2$ is $\{(i, j), (i, j-1)\} \preceq \{(i, h), (i, h-1)\}$ iff $j \leq h$. In this case, ρ must be a decreasing function of both its arguments. Moreover we require that $\frac{\partial^2 \rho}{\partial b_1 \, \partial b_2}(b_1, b_2) \neq 0$, so that there exists a real interaction between the involved discontinuities.

In our applications, we take

$$\rho(b_1, b_2) = \varepsilon \, (1 - b_1) \, (1 - b_2), \tag{4}$$

where ε is a positive parameter.

3 The dual energy function

To minimize the primal energy function, we first minimize with respect to all line variables b. In order to do this, we define the *dual energy function* as follows:

$$E_d(\boldsymbol{x}) = \inf_{\boldsymbol{b} \in B^{|C_k|}} E(\boldsymbol{x}, \boldsymbol{b}),$$

where the symbol $|C_k|$ denotes the cardinality of the set C_k. Let us consider for the moment the case $Q = 0$. The function E_d can be written as:

$$E_d(\boldsymbol{x}) = \|\boldsymbol{y} - A\boldsymbol{x}\|^2 + \sum_{c \in C_k} g(D_c^k(\boldsymbol{x})), \tag{5}$$

where $g(t) = \inf_{b \in B}\{\lambda^2\, b\, t^2 + \beta(b)\}$ is called *the interaction function.* When B and β are as in (2), then

$$g(t) = \min\{\lambda^2\, t^2, \alpha\} = \begin{cases} \lambda^2 t^2 & \text{if } |t| < \sqrt{\alpha}/\lambda \\ \alpha & \text{otherwise.} \end{cases} \tag{6}$$

The quantity $s = \sqrt{\alpha}/\lambda$ has the meaning of a threshold for creating a discontinuity.

Geman and Reynolds [11] and Charbonnier, Blanc-Féraud, Aubert and Barlaud [8] proved two different versions of the duality theorem. This theorem gives a correspondence between the primal and dual energy functions. Anyway, in our context, Geman and Reynolds added the supplementary hypothesis that the limit of $g(t)$ is finite as t tends to infinity. On the other hand they did not give any regularity condition on the functions g and β. The function $g(t) = \min\{\lambda^2\, |t|, \alpha\}$, which satisfies all the assumptions of the duality theorem in [11], induces, however, line variables b which can assume value $+\infty$. Moreover, Charbonnier et al. gave particular hypotheses on the function g, which are not satisfied by the function given in (6).

Hence, we need a new version of the duality theorem, whose proof is given in [7].

Theorem 3.1 *Fix $\lambda \neq 0$, and:*
a) let $B = \bigcup_{j=1}^{m} I_j$, where I_j is a bounded interval or a singleton contained in $[0, +\infty)$, $j = 1, \ldots, m$, and such that $\overline{I_j} \bigcap \overline{I_l} = \varnothing$ for every $j \neq l$;
b) let $\beta : B \to \mathbb{R}$ be a bounded from below, strictly decreasing, continuous function on B, which is strictly convex on each interval I_j.

Define

$$g(t) = \inf_{b \in B}\{\lambda^2\, b\, t^2 + \beta(b)\},\ t \in \mathbb{R}. \tag{7}$$

Then

c) the function g is even in $\mathbb{R}$, nondecreasing on $[0, +\infty)$ and of class $\mathrm{Lip}_{\mathrm{loc}}(\mathbb{R})$;

d) the function $f(t) = g(\sqrt{t})$, $t \geq 0$, is nondecreasing, continuous and concave on $[0, +\infty)$, and possibly not differentiable at most finitely many points of $(0, +\infty)$. Moreover, f' is nonincreasing and continuous on its domain, and

$$f(0) = \lim_{b \to \sup B} \beta(b).$$

Conversely, if $g : \mathbb{R} \to \mathbb{R}$ and $f : [0, +\infty) \to \mathbb{R}$ are two functions, satisfying c) and d), respectively, then there exist a set $B \subset [0, +\infty)$ and a function $\beta : B \to \mathbb{R}$, satisfying a), b) and (7).

Now, let us consider the case $Q \neq 0$. In particular let Q be as in (3), where the corresponding function ρ has the property that its mixed second derivative never vanishes. In this case, it is difficult to compute explicitly the duality energy function, and so we consider an approximation $\xi_{c-1}(\boldsymbol{x})$ of the variable b_{c-1}, defined as:

$$\xi_{c-1}(\boldsymbol{x}) = \arg_{c-1} \min_{\boldsymbol{b} \in B^{|C_k|}} E(\boldsymbol{x}, \boldsymbol{b}) = \arg \min_{b \in B} \{\lambda^2 D^k_{c-1}(\boldsymbol{x}) b + \beta(b)\}, \tag{8}$$

where E is as in (1). Of course, ξ_{c-1} depends only on $D^k_{c-1}(\boldsymbol{x})$, so, without loss of generality, we can write $\xi_{c-1}(\boldsymbol{x}) = \mu(D^k_{c-1}(\boldsymbol{x}))$. Now we define the primal energy as follows:

$$E(\boldsymbol{x}, \boldsymbol{b}) = \|\boldsymbol{y} - A\boldsymbol{x}\|^2 + \sum_{c \in C_k} \left[\lambda^2 (D^k_c \boldsymbol{x})^2 b_c + \beta(b_c) + \rho(b_c, \mu(D^k_{c-1}(\boldsymbol{x})))\right],$$

with the convention that, if $c - 1$ does not exist, then $\rho(b_c, \mu(D^k_{c-1}(\boldsymbol{x}))) = 0$. The corresponding dual energy is

$$E_d(\boldsymbol{x}) = \|\boldsymbol{y} - A\boldsymbol{x}\|^2 + \sum_{c \in C_k} \psi(D^k_c(\boldsymbol{x}), D^k_{c-1}(\boldsymbol{x})), \tag{9}$$

where

$$\psi(t_1, t_2) = \inf_{b \in B} \{\lambda^2 b t_1^2 + \beta(b) + \rho(b, \mu(t_2))\}.$$

In the particular case in which B, β and ρ are as in (2) and (4) respectively, we have that $\mu(t) = 1$ if $|t| < s$, $s = \sqrt{\alpha}/\lambda$, and $\mu(t) = 0$ otherwise. Hence we get

$$\psi(t_1, t_2) = \begin{cases} \begin{cases} \lambda^2 t_1^2 & \text{if } |t_1| < s \\ \alpha & \text{if } |t_1| \geq s \end{cases} & \text{if } |t_2| < s \\ \begin{cases} \lambda^2 t_1^2 & \text{if } |t_1| < \sqrt{\alpha + \varepsilon}/\lambda \\ \alpha + \varepsilon & \text{if } |t_1| \geq \sqrt{\alpha + \varepsilon}/\lambda \end{cases} & \text{if } |t_2| \geq s \end{cases} \tag{10}$$

4 GNC algorithms

In this section we present an algorithm to minimize the dual energy E_d. In general, E_d is not convex. The algorithms for minimizing a function, when it is not convex, depend on the choice of the starting point. To give an adequate choice of the initial point, a standard technique is to find a finite family of approximating functions $\{E_d^{(p)}\}_p$, such that the first is convex and the last is the original dual energy function [1, 2, 5, 6, 12], and then to apply the following algorithm:

initialize $\boldsymbol{x}$;
while $E_d^{(p)} \neq E_d$ do

- find the minimum of the function $E_d^{(p)}$ starting from the initial point $\boldsymbol{x}$;
- $\boldsymbol{x} = \arg\min E_d^{(p)}$;
- update the parameter p.

Such an algorithm is called GNC (Graduated Non-Convexity) algorithm. The first GNC algorithm was proposed by Blake and Zisserman [5, 6], who approximate the dual energy in (5) where the function g is defined in (6), with $A = I$ and I is the identity matrix. Bedini, Gerace and Tonazzini [2] proposed an extension of GNC algorithm, called E-GNC, for the dual energy given in (9), ψ in (10) and $A = I$, which takes into account the constraints of non-parallelism. Moreover, Nikolova [12] studied the dual energy in (5), where g is given as in (6), but A is an arbitrary blur matrix, not necessarily close to the identity matrix.

5 The CATILED algorithm

Here, we focus our attention on finding a family of approximating functions of the dual energy function (9), where ψ is given as in (10) and A is an arbitrary matrix. Thus we deal with the problem of deblurring, which takes into account the constraints of non-parallelism. The Hessian matrix associated with faithfulness to data in (9) is $2\,A^T\,A$, and so it is positive semidefinite.

We now deal with the problem of finding a convex approximation of the regularization term in (9) in the case $k = 1$. Given a clique $c \in C_1$ such that $c-1$ exists, set $n_1(c) = c \setminus (c-1)$, $n_2(c) = c \bigcap (c-1)$ and $n_3(c) = (c-1) \setminus c$. We observe that $n_l(c)$, $l = 1, 2, 3$, are singletons and that $D_c^1(\boldsymbol{x}) = x_{n_1(c)} - x_{n_2(c)}$,

$D^1_{c-1}(\boldsymbol{x}) = x_{n_2(c)} - x_{n_3(c)}$. Let ψ^* be a first convex approximation of ψ of class $C^1(\mathbb{R}^2)$. In this paper, for simplicity, we take the following specific first convex approximation ψ^* of (10), defined by

$$\psi^*(t_1) = \psi^*(t_1, t_2) \;=\; \begin{cases} \lambda^2 t_1^2 & \text{if } \mid t_1 \mid < q \\ \\ 2\,\lambda^2 q\,|t_1| - \lambda^2 q^2 & \text{if } \mid t_1 \mid \geq q \end{cases} \qquad \forall\, t_2 \in \mathbb{R}, \tag{11}$$

where $q = \frac{\sqrt{\alpha}}{\lambda^2}\left(\frac{2}{\tau^*} + \frac{1}{\lambda^2}\right)^{-1/2}$, and τ^* is an arbitrary positive real constant, whose role will be clarified below. Of course $\psi^* = \psi^*(t)$ is trivially convex in $\mathbb{R}$.

For $p = 0$ then $\psi^{(}0) \equiv \psi$.

For $p \in (0, 1]$, let the approximating functions be

$$\psi^{(p)}(t_1, t_2) \;=\; \begin{cases} g^{(p)}(t_1, \alpha) \\ \qquad\qquad \text{if} \quad \mid t_2 \mid \leq s \\ \\ a^{(p)}(t_1)(\mid t_2 \mid -s)^2 + g^{(p)}(t_1, \alpha) \\ \qquad\qquad \text{if} \quad s < \mid t_2 \mid \leq \dfrac{u(p) + s}{2} \\ \\ -a^{(p)}(t_1)(\mid t_2 \mid -u(p))^2 + g^{(p)}(t_1, \alpha + \varepsilon) \\ \qquad\qquad \text{if} \quad \dfrac{u(p) + s}{2} < \mid t_2 \mid < u(p) \\ \\ g^{(p)}(t_1, \alpha + \varepsilon) \\ \qquad\qquad \text{otherwise,} \end{cases} \tag{12}$$

where $u(p) = s + pz$, with z an arbitrary positive real number, which will be determined later, where

$$g^{(p)}(t, \alpha) \;=\; \begin{cases} \lambda^2 t^2 & \text{if} \quad \mid t \mid < q \\ \alpha - (\tau/2)(\mid t \mid - r)^2 & \text{if} \quad q \leq \mid t \mid \leq r \\ \alpha & \text{if} \quad \mid t \mid > r, \end{cases} \quad , \quad \tau = \frac{\tau^*}{p},\, r = \frac{\alpha}{\lambda^2 q},$$

and where finally

$$a^{(p)}(t) = 2\frac{g^{(p)}(t, \alpha + \varepsilon) - g^{(p)}(t, \alpha)}{[u(p) - s]^2}.$$

For $p \in [1, 2]$, the approximating function is defined by

$$\psi^{(p)} = (p - 1)\,\psi^* + (2 - p)\psi^{(1)},$$

where ψ^* and $\psi^{(1)}$ are given in (11) and (12). In our GNC algorithm, the parameter p varies linearly from 2 to 0. In Figure 1 there are the graphs of the functions $\psi^{(2)} \equiv \psi^*$, $\psi^{(1)}$ and $\psi^{(0)} \equiv \psi$. Note that the presence of z and τ^* makes the approximation functions $\psi^{(p)}$ of class $C^1(\mathbb{R}^2)$, for all $p \in (0, 2]$, as required in the numerical algorithm. For the sake of simplicity, we refer our algorithm as CATILED (Convex Approximation Technique for Interacting Line Elements Deblurring). When $\varepsilon = 0$ the family of approximations $\psi^{(p)}$ is exactly the one given by Nikolova [12].

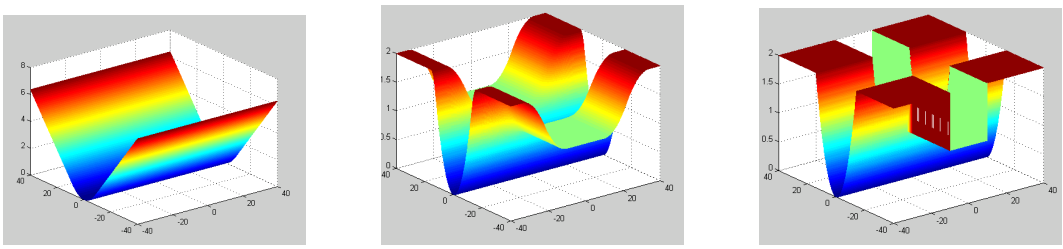

Figure 1: On the left, middle and right side there are the functions $\psi^{(2)} \equiv \psi^*$, $\psi^{(1)}$ and $\psi^{(0)} \equiv \psi$ respectively (obtained with $\lambda = 0.1$, $\alpha = 1$ and $\varepsilon = 1$).

6 Primal energy function of the first convex approximation

Let ψ^* be the first convex approximation function given in (11), take $g^*(t) = \psi^*(t)$, $t \in \mathbb{R}$, and $f^*(t) = g^*(\sqrt{t})$ for all $t \geq 0$. Hence, by direct calculation, f^* and g^* satisfy the conditions c) and d) of the duality theorem, so that they are adequate to deal with implicit discontinuities. We can construct the set B^* and the function β^* satisfying a), b) and (7) of the duality theorem. Indeed, following the proof of the duality theorem (see [7]), we put $B^* = \left\{ \frac{\zeta}{\lambda^2} : \zeta \in \Xi \right\}$, where Ξ is the set of the values attained by $f^{*\prime}$, in other words $B^* = (0, 1]$. The function $\beta^*(b)$, $b \in B^*$, is the y-coordinate of the intersection point between the y-axis and any tangent line to the graph of f^* whose angular coefficient is $\lambda^2\, b$. The function β^* is well-defined by

$$\beta^*(b) = \lambda^2\, q^2\, (1/b - 1) \quad \forall\, b \in B^* = (0, 1].$$

In Figure 2 on the left, middle and right side there are the graphs of the functions g^*, f^*, β^* respectively.

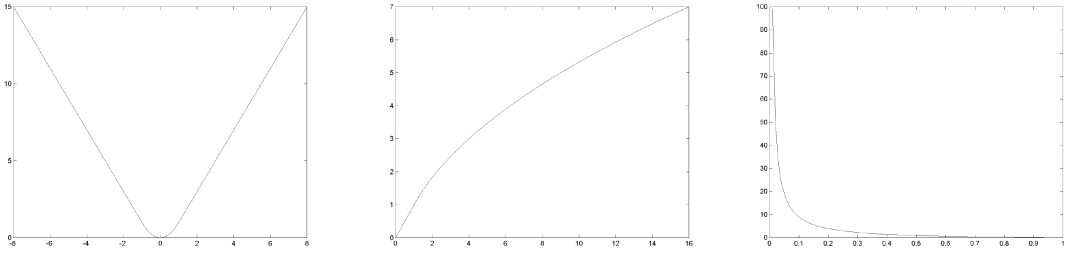

Figure 2: On the left, middle and right side there are the graphs of the functions g^*, f^*, β^* respectively, (obtained with $\lambda = 1$ and $q = 1$)

7 Experimental results

In this section we compare, by some experimental results, the performance of the algorithms GNC given by Blake and Zisserman [6], E-GNC [2] and CATILED. These algorithms are tested considering both syntetic piecewise smooth and real images as original ones. The degraded images are obtained by applying the blur matrix and sometimes by adding a white Gaussian noise. The family of the approximations of dual energy is minimized according to the Successive Over-Relaxation (SOR) algorithm. The parameters α, λ and ε are chosen experimentally. In Figure 3, on the left side there is the first considered 128×128 image (syntetic1). On the right side there is the image syntetic1 blurred by

$$M = \frac{1}{25} \begin{pmatrix} 1 & 1 & 1 & 1 & 1 \\ 1 & 1 & 1 & 1 & 1 \\ 1 & 1 & 1 & 1 & 1 \\ 1 & 1 & 1 & 1 & 1 \\ 1 & 1 & 1 & 1 & 1 \end{pmatrix}. \tag{13}$$

In Figure 4, on the left, middle and right side there is the restoration by GNC, E-GNC and CATILED respectively. The parameters that we use for all algorithms are $\lambda = 0.5$ and $\alpha = 10$. Moreover, for the algorithms E-GNC and CATILED, we set $\varepsilon = 150$. In Figure 5, there are the respective variable elements of the images in Figure 4. We present the images relative to line elements in order to show how CATILED avoids parallel lines better than the other two algorithms. In Figure 6, on the left side there is the second considered 160×160 image (syntetic2). On the right side there is the image

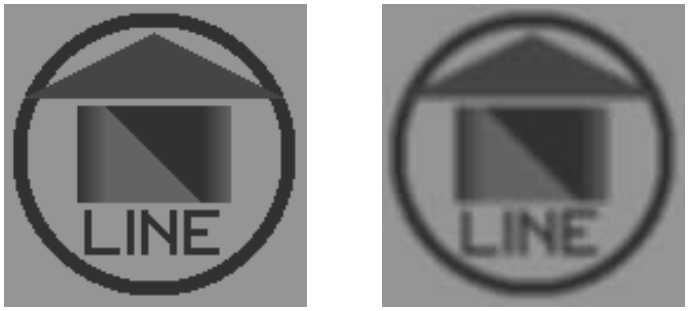

Figure 3: The image on the left side is the image syntetic1; the image on the right is the image blurred by mask (13).

Figure 4: Image syntetic1 restored by GNC, E-GNC and CATILED respectively.

syntetic2 blurred by

$$M = \frac{1}{430}\begin{pmatrix} 0 & 5 & 10 & 5 & 0 \\ 5 & 25 & 50 & 25 & 5 \\ 10 & 50 & 50 & 50 & 10 \\ 5 & 25 & 50 & 25 & 5 \\ 0 & 5 & 10 & 5 & 0 \end{pmatrix} \tag{14}$$

and corrupted by Gaussian white noise with $\sigma^2 = 100$. In Figure 7, on the left, middle and right side there is the restoration by GNC, E-GNC and CATILED respectively. The parameters that we use for all algorithms are $\lambda = 4$ and $\alpha = 1200$. For the algorithms E-GNC and CATILED we set $\varepsilon = 1200$. In Figure 8, there are the respective variable elements of the images in Figure 7. In Figure 9, on the left side there is the third considered 32×32 image (syntetic3). On the right side there is the image syntetic3 blurred by the mask M given in (13). In Figure 10, on the left, middle and right side there is the

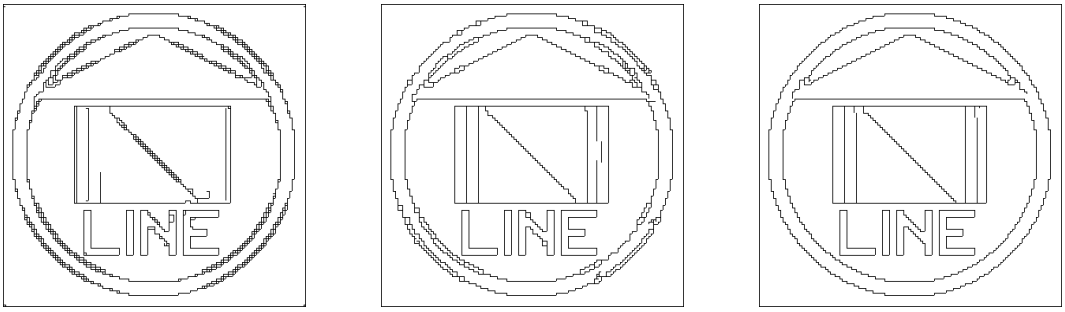

Figure 5: Line variables of the image syntetic1 restored by GNC, E-GNC and CATILED respectively.

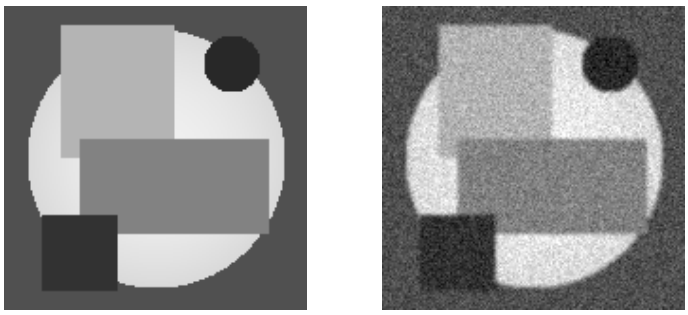

Figure 6: The image on the left side is the image syntetic2; the image on the right is the image blurred by mask (14) and corrupted by Gaussian noise.

restoration by GNC, E-GNC and CATILED respectively. The parameters we use for all algorithms are $\lambda = 0.5$, $\alpha = 200$ and, for the algorithms E-GNC and CATILED, $\varepsilon = 400$. In Table 1 there are the mean squared error (MSE) between the reconstructed images and the original ones. In Figure 11, on the left side there is the last presented 222×222 image (real1). On the middle side there is the image real1 blurred by the mask M given in (13). On the right side there is the image restored by CATILED. The used parameters are $\lambda = 0.5$, $\alpha = 1$, $\varepsilon = 3$.

References

[1] L. Bedini, I. Gerace, E. Salerno, A. Tonazzini, Models and Algorithms for Edge-Preserving Image Reconstruction. Advances in Imaging and Electron Physics. 97 (1996) 86–189.

Figure 7: Image syntetic2 restored by GNC, E-GNC and CATILED respectively.

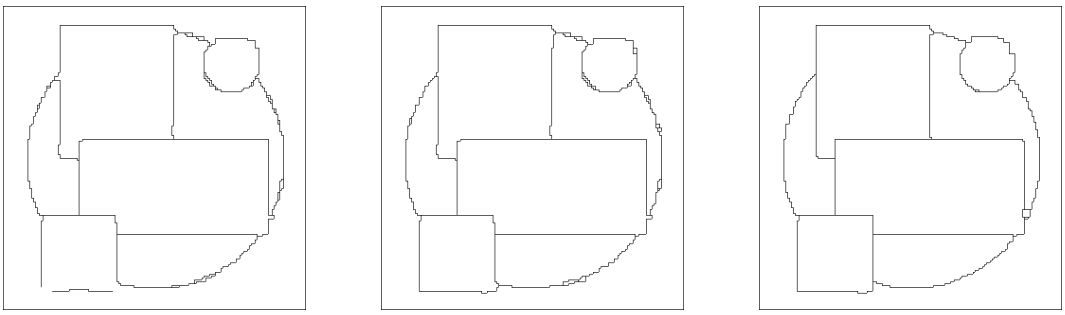

Figure 8: Line variables of the image syntetic2 restored by GNC, E-GNC and CATILED respectively.

[2] L. Bedini, I. Gerace, A. Tonazzini, A Deterministic Algorithm for Reconstruction Images with Interacting Discontinuities. CVGIP: Graphical Models Image Process. 56 (1994) 109–123.

[3] M. Bertero, P. Boccacci, *Introduction to Inverse Problems in Imaging.* Institute of Physics Publishing, Bristol and Philadelphia, 1998.

[4] M. Bertero, T. Poggio, V. Torre, Ill-Posed Problems in Early Vision. IEEE Proc. 76 (1988) 869–889.

[5] A. Blake, Comparison of the Efficiency of Deterministic and Stochastic Algorithms for Visual Reconstruction. IEEE Trans. Pattern Anal. Machine Intell. 11 (1989) 2–12.

[6] A. Blake, A. Zisserman, *Visual Reconstruction.* MIT Press, Cambridge, MA, 1987.

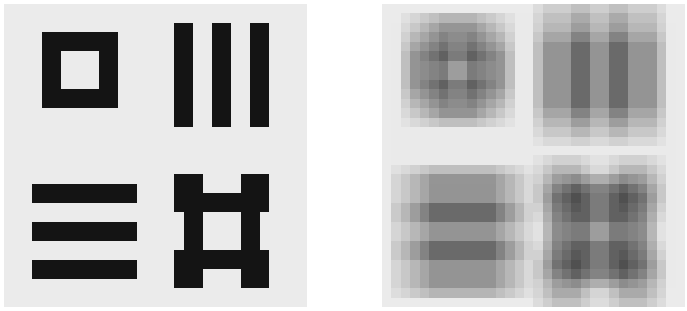

Figure 9: The image on the left side is the image syntetic3; the image on the right side is the image blurred by (13).

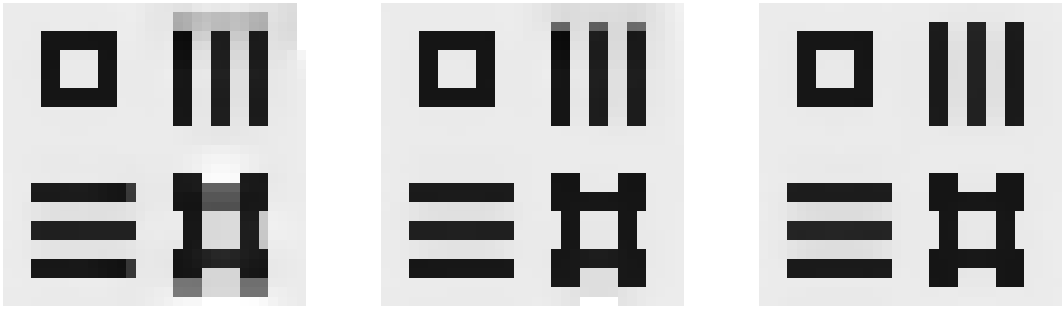

Figure 10: Image syntetic3 restored by GNC, E-GNC and CATILED respectively.

[7] A. Boccuto, M. Discepoli, I. Gerace, R. Pandolfi, P. Pucci, Tecniche di Minimizzazione Gradualmente Non Convesse per il Restauro di Immagini Sfuocate. Rapporto Tecnico n. 16, Dip. Matematica e Informatica, Univ. Perugia (2002).

[8] P. Charbonnier, L. Blanc-Féraud, G. Aubert, M. Barlaud, Deterministic Edge-Preserving Regularization in Computed Imaging. IEEE Trans. Image Process. 6 (1997) 298–311.

[9] G. Demoment, Image Reconstruction and Restoration: Overview of Common Estimation Structures and Problems. IEEE Trans. Acoust., Speech, and Signal processing. 37 (1989) 2024–2036.

[10] S. Geman, D. Geman, Stochastic Relaxation, Gibbs Distributions, and the Bayesian Restoration of Images. IEEE Trans. Patt. Anal. Machine Intell. 6 (1984) 721–740.

Algorithm	Syntetic1	Syntetic2	Syntetic3
GNC	3.83	7.60	21.74
E-GNC	8.57	8.70	8.04
CATILED	2.41	6	5.20

Table 1: Mean squared error (MSE) between the restored images and the original ones.

Figure 11: On the left, middle and right side there are the image real1, the image blurred by (13) and the image restored by CATILED.

[11] D. Geman, G. Reynolds, Constrained Restoration and the Recovery of Discontinuities. IEEE Trans. Pattern Anal. Machine Intell. 14 (1992) 367–383.

[12] M. Nikolova, (1999) Markovian Reconstruction Using a GNC Approach. IEEE Trans. Image Process. 8 (1999) 1204–1220.